

# High-resolution Hybrid Inversion of IASI Ammonia Columns to Constrain U.S. Ammonia Emissions Using the CMAQ Adjoint Model

Yilin Chen<sup>1</sup>, Huizhong Shen<sup>1</sup>, Jennifer Kaiser<sup>1,2</sup>, Yongtao Hu<sup>1</sup>, Shannon L. Capps<sup>3</sup>, Shunliu Zhao<sup>4</sup>, Amir Hakami<sup>4</sup>, Jih-Shyang Shih<sup>5</sup>, Gertrude K. Pavur<sup>1</sup>, Matthew D. Turner<sup>6</sup>, Daven K. Henze<sup>7</sup>, Jaroslav Resler<sup>8</sup>, Athanasios Nenes<sup>9,10</sup>, Sergey L. Napelenok<sup>11</sup>, Jesse O. Bash<sup>11</sup>, Kathleen M. Fahey<sup>11</sup>, Gregory R. Carmichael<sup>12</sup>, Tianfeng Chai<sup>13</sup>, Lieven Clarisse<sup>14</sup>, Pierre-François Coheur<sup>14</sup>, Martin Van Damme<sup>14</sup>, Armistead G. Russell<sup>1</sup>

<sup>1</sup>School of Civil and Environmental Engineering, Georgia Institute of Technology, Atlanta, Georgia 30332, United States

<sup>2</sup>School of Earth and Atmospheric Sciences, Georgia Institute of Technology, Atlanta, Georgia 30332, United States

<sup>3</sup>Department of Civil, Architectural, and Environmental Engineering, Drexel University, Philadelphia, Pennsylvania 19104, United States

<sup>4</sup>Department of Civil and Environmental Engineering, Carleton University, Ottawa, Ontario K1S5B6, Canada

<sup>5</sup>Resources for the Future, Washington, D.C. 20036, USA

<sup>6</sup>SAIC, Stennis Space Center, MS 39529, USA

<sup>7</sup>Mechanical Engineering Department, University of Colorado, Boulder, CO 80309, USA

<sup>8</sup>Institute of Computer Science of the Czech Academy of Sciences, Prague, 182 07, Czech Republic

<sup>9</sup>Institute for Chemical Engineering Sciences, Foundation for Research and Technology Hellas, Patras, GR-26504, Greece

<sup>10</sup>School of Architecture, Civil & Environmental Engineering, Ecole polytechnique fédérale de Lausanne, CH-1015, Lausanne, Switzerland

<sup>11</sup>Atmospheric & Environmental Systems Modeling Division, U.S. EPA, Research Triangle Park, NC 27711, USA

<sup>12</sup>Department of Chemical and Biochemical Engineering, University of Iowa, Iowa City, IA 52242, USA

<sup>13</sup>NOAA Air Resources Laboratory (ARL), Cooperative Institute for Satellites Earth System Studies (CISESS), University of Maryland, College Park, MD 20740, USA

<sup>14</sup>Université libre de Bruxelles (ULB), Spectroscopy, Quantum Chemistry and Atmospheric Remote Sensing (SQUARES), Brussels, Belgium

*Correspondence to:* Armistead G. Russell (ar70@ce.gatech.edu)

**This material includes 5 figures.**

## List of Figures

**S1.** The correlation between monthly average CMAQ simulated NH<sub>3</sub> column densities and NH<sub>3</sub> concentrations at all 13 layers in April, July, and October.

**S2.** The L-curve for regularization factor ( $\gamma$ ) value selection for April, July, and October.

**S3.** Comparison between simulated NH<sub>3</sub> column density against the IASI-NH<sub>3</sub> observations in April, July, and October using *a priori* (blue dots) and optimized NH<sub>3</sub> emission estimates (red dots).

**S4.** IASI NH<sub>3</sub> column density in April 13<sup>th</sup>, 14<sup>th</sup>, and 15<sup>th</sup> at 36 m by 36 km resolution within the model simulation domain of this study.

**S5.** Protected areas for biodiversity conservation defined by the U.S. Geological Survey (USGS) Gap Analysis Project (A). And fraction of protected areas in each 36 km by 36 km simulated grids in this study (B).

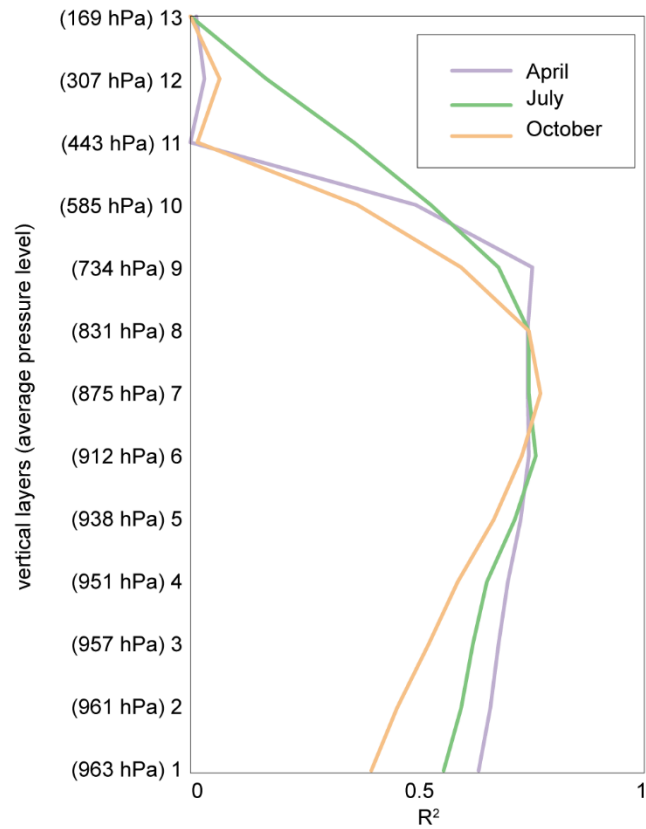


**Figure S1** The correlation between monthly average CMAQ simulated NH<sub>3</sub> column densities and NH<sub>3</sub> concentrations at all 13 layers in April, July, and October. The grid cells with satellite observations are sampled at the IASI overpassing time. Monthly average NH<sub>3</sub> column densities and concentrations are calculated for each grid cell. R<sup>2</sup> for all data pairs in each month are calculated.

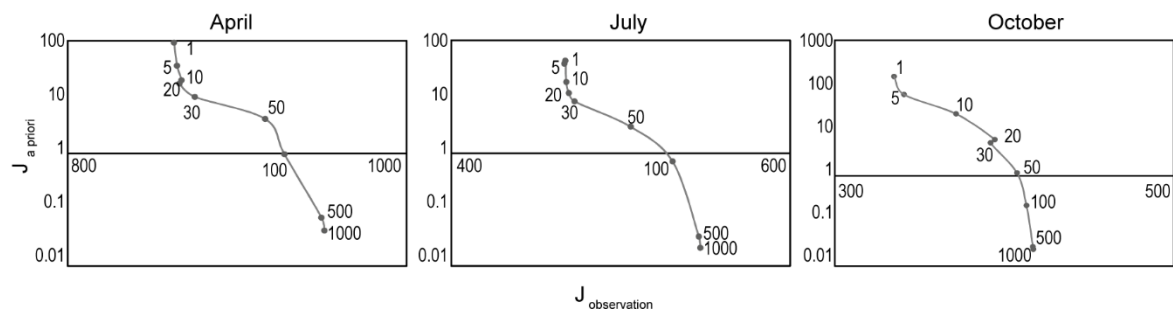


**Figure S2** The L-curve for regularization factor ( $\gamma$ ) value selection for April, July, and October. The error weighted squared difference between emission scaling factor and the a priori values ( $J_{a\text{ priori}}$ ) is plotted against error weighted squared difference between IASI-NH<sub>3</sub> and simulated column density ( $J_{\text{observation}}$ ) with different choices of  $\gamma$  values as denoted along the curve.

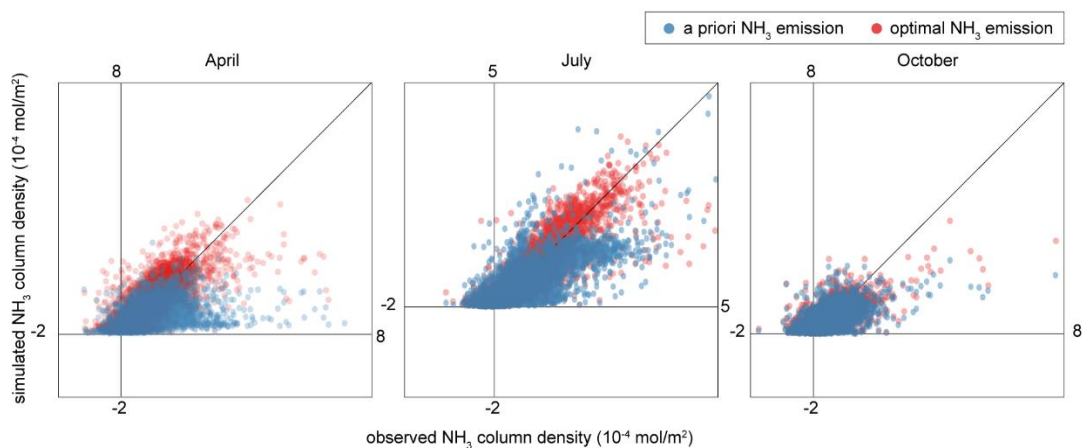


**Figure S3** Comparison between simulated NH<sub>3</sub> column density against the IASI-NH<sub>3</sub> observations in April, July, and October using a priori (blue dots) and optimized NH<sub>3</sub> emission estimates (red dots).

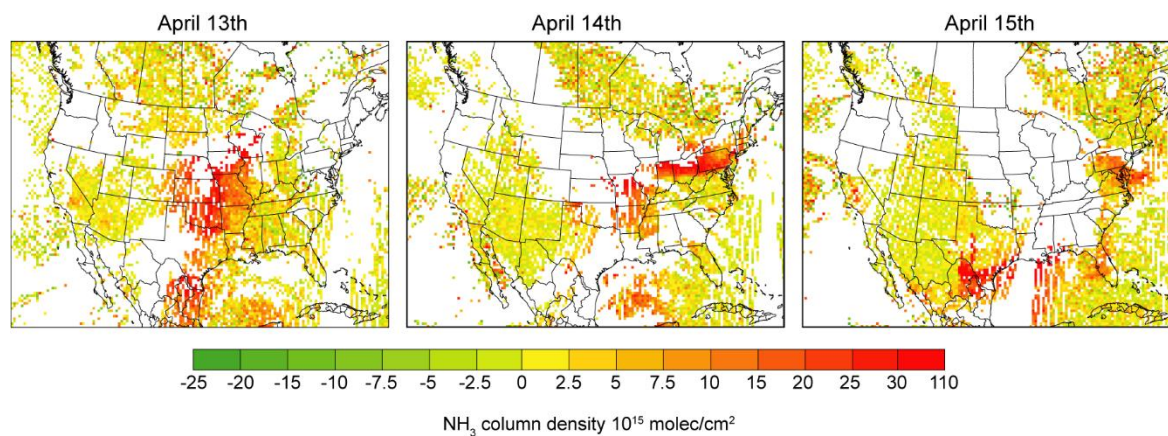


**Figure S4** IASI NH<sub>3</sub> column density in April 13<sup>th</sup>, 14<sup>th</sup>, and 15<sup>th</sup> at 36 m by 36 km resolution within the model simulation domain of this study.

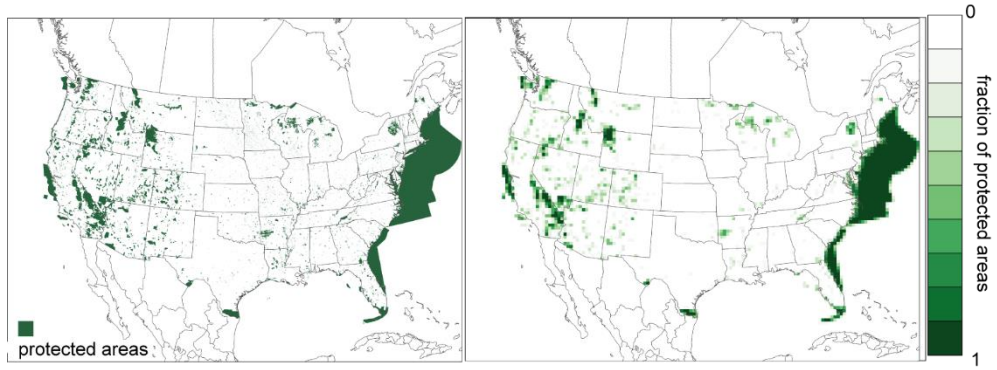


**Figure S5** Protected areas for biodiversity conservation defined by the U.S. Geological Survey (USGS) Gap Analysis Project (A). And fraction of protected areas in each 36 km by 36 km simulated grids in this study (B).